Hydrogenic Binding Energy, Carrier Concentration, and Mobility Calculations for Quantum Wires

Qin Zhang, Anubhav Khandelwal, and Jeffrey Bean
Department of Electrical Engineering, University of Notre Dame, Notre Dame, Indiana 46656

Abstract: Hydrogenic impurity binding energy in a quantum wire is studied as a function of the wire dimension and impurity position with respect to the wire axis. Variational wavefunction is used to account for the electron confinement within the wire. The electron carrier density is calculated from the impurity binding energy, which is a function of wire radius, temperature, and doping density. Finally, the surface roughness limited momentum relaxation time is derived and its effect on mobility is analyzed.

The electronics industry continues to move toward increased performance by the continued miniaturization of current devices, using Moore's Law as a guide.[1] As the fundamental limits of these devices have come into view in the foreseeable future, structures that will replace or augment current technologies have been a source for increased research efforts.[2,3] Over recent years, as miniaturization reaches towards the fundamental limits of size on current technologies, researchers and industry began to study and find viable structures to replace or augment existing devices. Some of these exotic devices employ the use of one dimensional structures, such as nanowires.[4-7]

However, the aforementioned structures exhibit electrical and mechanical properties that are much different that that of a bulk, three-dimensional material.[9,10] As a semiconductor structure is confined in multiple dimensions, quantum effects begin to change the electrical properties, including band gap.[11-14] The study of size quantization is attractive because it can reveal confined particle behavior. Nanowires exhibit strong finite-size effects on transport properties as the mobile carrier mean-free path is limited by the size of the wire.[15] Issues such as the band gap variation with size and impurity binding energy as a function of wire size and dopant position in have been well studied.[11,16] Carrier mobility in nanowires has also been studied.[17-21]

The calculation of the impurity binding energies has been performed assuming an infinite potential boundary condition using a variational wave function. The effective mass approximation is used to develop the Hamiltonian. Nanowires are assumed to be cylindrical to best approximate real wires as well as to reduce numerical integration. Impurity binding energies, thus calculated, are used to determine the ionized carriers in the conduction band. Mobility in nanowires is then studied, taking surface roughness into consideration.

For the case of our calculations, we assume the quantum wire to have no cladding, therefore being surrounded by air. In this project, the effective mass approximation will be used to determine the effect of size on the band gap.

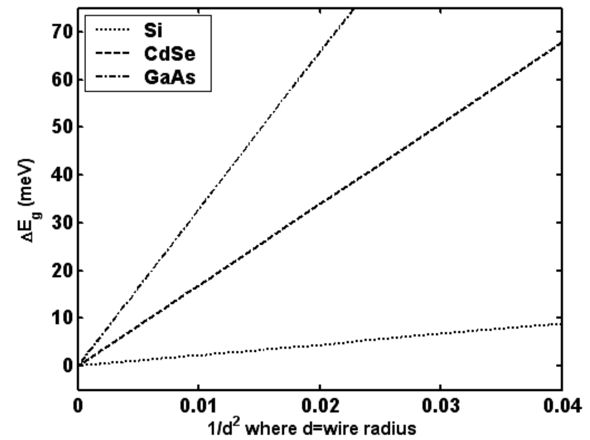

Fig. 1. Electronic Band Gap Variation vs. wire radius *d* (nm).

Due to the aforesaid quantum effects as a structure is confined in multiple dimensions, the energy band gap rises. This is due to the energy quantization that occurs when the material under confinement.

This size dependence will also be applied to the binding energy of hydrogenic impurity dopant atoms. The binding energy of hydrogenic impurities within a nanowire has been studied extensively in terms the quantum wire radius as well as the position of the dopant inside the wire.[22-24]

IMPURITY BINDING ENERGY

We have calculated the binding energy using the expression (derived by Jerry Brown and Harold Spector):

$$E_b(d,\rho_o) = -(\lambda a)^2 - 4a\frac{B}{dB/d\lambda}$$

Where $B = \int_0^1 dt t J_0^{\,2}(xt) I_0(2\lambda a y t_{<}) K_0(2\lambda a y t_{>})$

We have considered the cases when impurity is located on the axis, on the edge, and at the centre of the axis and edge ($t_0=0$, ½, 1 respectively) for different values of d[22].

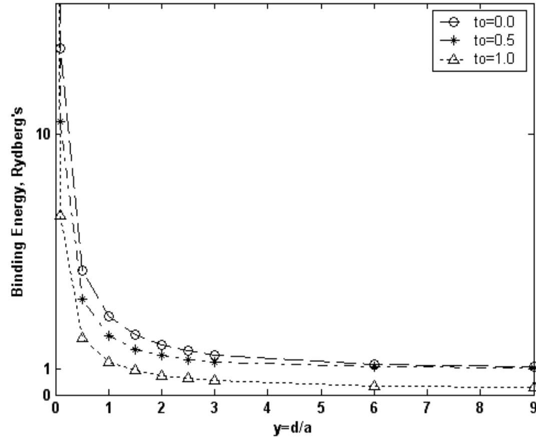

Fig. 2. Rydberg Normalized Binding Energy vs Normalized y for three different impurity positions in the wire.

From Figure 2, it is clear that when the impurity is present inside the wire (ρ<d), as we make d larger, $E_b(d,\rho_0)$ attains a constant value equal to *R*, which is the limit for 3 dimensional hydrogen case. As we make *d* comparable to *a*, more confinement of particle result in an increase in binding energy and it keeps on increasing as d is reduced. Further, as impurity position moves away from the axis, $E_b(d,\rho_0)$ decreases and is maximum when the particle is on the axis $\rho_0 = 0$.

We have determined the hydrogenic binding energies for Si, GaAs and CdSe using parameters as listed below[8].

	m_e^*/m_0	$\varepsilon/\varepsilon_0$	a_0^*(nm)	R_0^*(meV)
Si	0.98	11.7	0.63	978
GaAs	0.063	12.9	10.78	52
CdSe	0.13	10.2	4.13	17

Table 1. Parameters for Si, GaAs, CdSe (used in simulation)

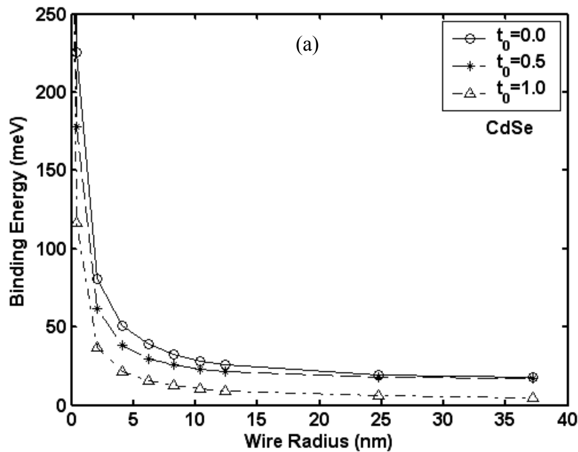

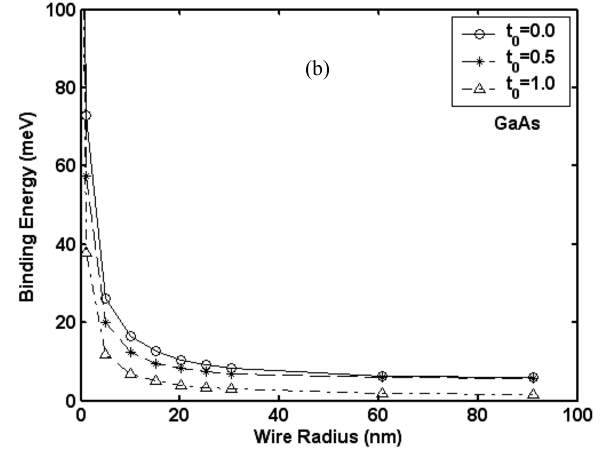

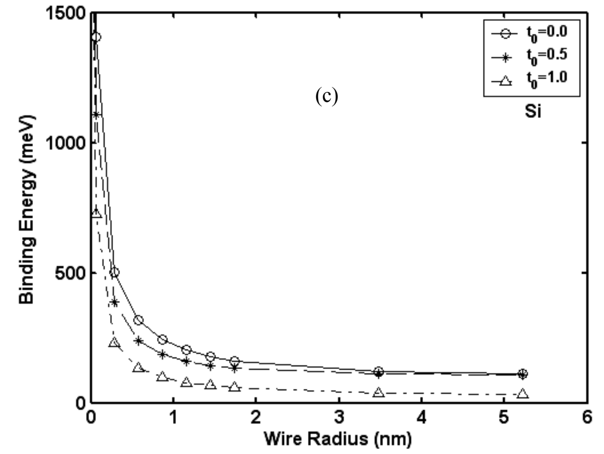

Fig. 3. Binding energy vs. Wire radius for (a) CdSe (b) GaAs and (c) Si

Note: The effective mass approximation breaks down for very thin wires.[23] From Fig. 3, when *d* is 5nm, the binding energy for GaAs is less than 25meV, for CdSe it is less than 45meV and for Si it is less than 200meV. +It is clear that it is easier to dope a material with smaller effective mass. And material with large effective mass, like Si, it is difficult to observe quantum confinement effects even in wire with radius as small as 2.5nm.

CARRIER CONCENTRATION

For the 1-D case, the total electron concentration in the conduction band is:

$$n^{1D} = \int_{E_c}^{E_{top}} g_c^{1D}(E) f(E) dE ,$$

where $g_c^{1D}(E)$ is the density of states (DOS) for 1-D and $f(E)$ is the Fermi distribution function.

Under non-degenerate conditions,

$$n^{1D} = N_C^{1D} \exp(-\frac{E_c - E_F}{kT}) ,$$

where $N_C^{1D} = \frac{\sqrt{2m_e^* kT}}{\sqrt{\pi}\hbar}$ is the 1-D effective density of conduction band states.

Using the charge-neutral relationship for n-type material:

$$n \approx N_D^+ ,$$

we find $n(E_b)$ (see Appendix A). Since E_b depends on the position of impurities, n need to be averaged:

$$< n >= \frac{\int_0^d n(\rho_0) 2\pi\rho_0 d\rho_0}{\int_0^d 2\pi\rho_0 d\rho_0} = \frac{2}{d^2}\int_0^d n(\rho_0)\rho_0 d\rho_0 ,$$

which is solved numerically. Here we assume the doping is uniform along the axis of the nanowires.

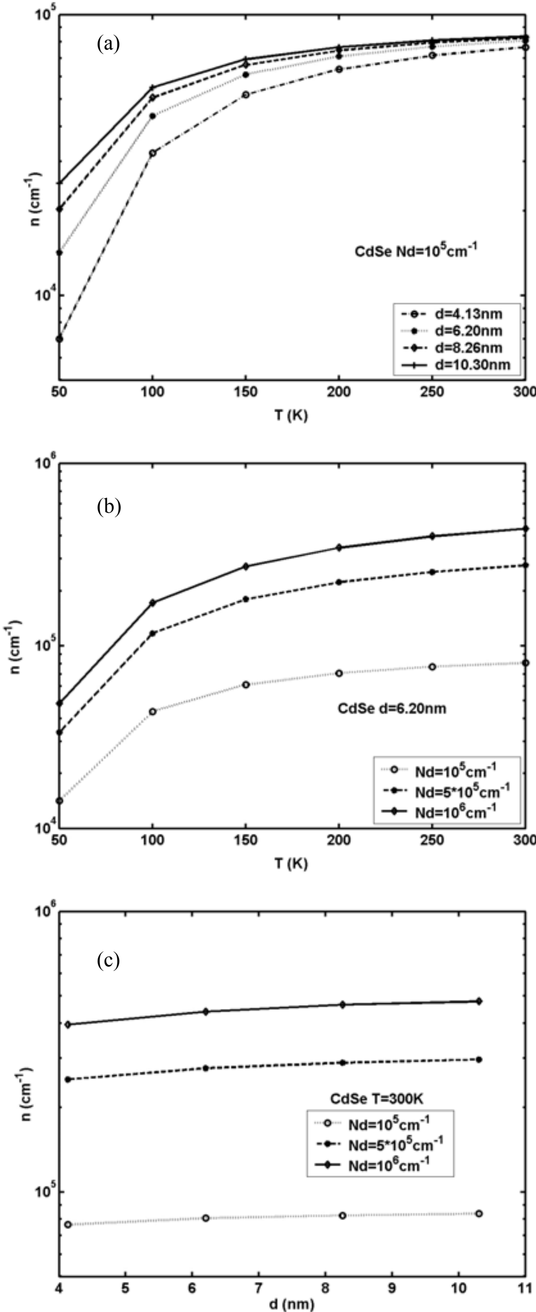

Fig. 4. Electron concentrations in the conduction band of CdSe: (a) *n* vs. temperature with different wire radius; (b) *n* vs. temperature with different doping; (c) *n* vs. wire radius with different doping.

Figure 4 shows the variations of electron concentration in the conduction band with the wire radius, doping level, and temperature. Similar with the 3-D case, electron concentration increases with temperature and doping density. Electron concentration also increases with the wire radius, because the binding energy decreases, which makes the wire easier to dope.

Note that for the 3-D case, we assume that all the dopants are ionized at room temperature. But for the 1-D case, we can see clearly from Fig that the dopants are not ionized completely at room temperature, which will be responsible for the difficulty of doping nanowires. For example, when $N_d=10^5$/cm and d=6.20nm, the percentage of ionization is 80.7and the percentage decreases to 43.9 when N_d increases to 10^6/cm.

In the same way, we also calculate electron concentrations for GaAs and Si at room temperature, shown in Table 2.

n (cm^{-1})	$N_D=10^5$/cm	$N_D=5*10^5$/cm	$N_D=10^6$/cm
d=0.5a=5.39nm	8.03E+04	2.73E+05	4.33E+05
d=a=10.78nm	8.33E+04	2.93E+05	4.70E+05
d=1.5a=16.17nm	8.43E+04	3.01E+05	4.84E+05

(a)

n (cm^{-1})	$N_D=10^5$/cm	$N_D=5*10^5$/cm	$N_D=10^6$/cm
d=5nm	6.40E+04	2.03E+05	3.16E+05
d=10nm	6.40E+04	2.03E+05	3.16E+05
d=15nm	6.40E+04	2.03E+05	3.16E+05

(b)

Table 2. Electron concentrations in the conduction band of (a) GaAs and (b) Si with different wire radius and doping.

For GaAs, the electron concentration has similar variations with CdSe; but for Si, the electron concentrations do not change with wire radius (no quantum effect is observed when d is larger than 5nm), which is due to its large electron effective mass.

Figure 5 compares the electron concentrations for these three materials.

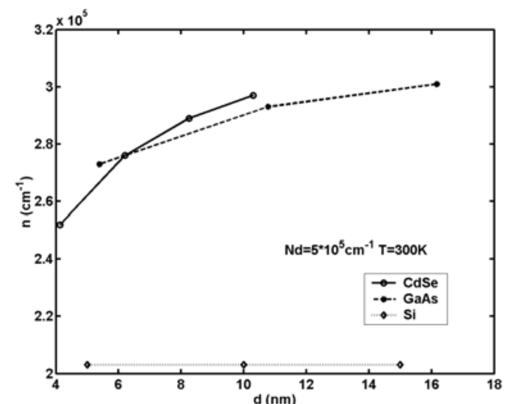

Figure 5. Electron concentration for CdSe, GaAs, and Si vs. wire radius with doping density of $5*10^5$/cm at 300K

It shows that Si has the lowest electron concentrations among the three at the same temperature and doping level, which is expected from its highest binding energy.

ROUGHNESS SCATTERING LIMITED MOMENTUM RELAXATION TIME:

For a quantum wire, confinement energy is given by $E = \frac{\hbar^2 k_{nl}^{\ 2}}{2m^*}$. For the ground state wave function $k_{10} = \frac{2.405}{d}$. Hence, E varies as d^{-2}. Roughness along the edges results in spatial variation of wire radius d and consequently variation in the confinement energy.

Roughness potential $V(r)$ is given by

$$V(r) = -\frac{\hbar^2 (2.405)^2}{m^* d^3} S(r),$$

where roughness $S(r)$ is assumed to be Gaussian and is expressed in terms of Δ (maximum height) and Λ (lateral variation) of the roughness s $S(r) = \Delta \exp(-\frac{z^2}{\Lambda^2})$,where Δ is the maximum height and Λ is the variation of the roughness. We assume roughness to be Gaussian, since it looks practical (is considered a good approximation for 2D quantum wells[25,26]), and includes both maximum height and lateral variation of roughness along the edges.

Using ground state wave-function for an electron, given by

$$\psi_{10k}(x) = \frac{e^{ikz} J_0(k_{10}\rho)}{(\pi d^2 L)^{1/2} J_1(k_{10} d)},$$

it can be shown (Appendix B) that the roughness scattering limited momentum relaxation time, assuming degeneracy, is given by

$$\tau_m = \frac{m^* d^6 k_F e^{2k_F^2 \Lambda^2}}{2\pi\hbar n (2.405)^4 \Delta^2 \Lambda^2},$$

where k_F is the Fermi wave vector given by $\pi n/2$ where n (per unit length) is the 1D carrier density (depends upon carriers due to ionized impurities, thermally generated or optically excited).

Mobility is than obtained by using the relation, $\mu = \frac{q\tau_m}{m^*}$.

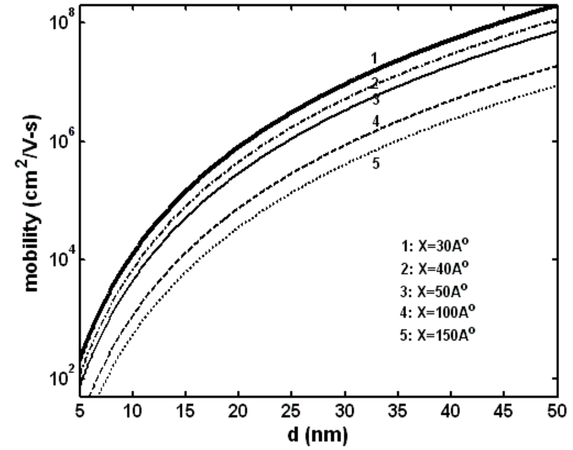

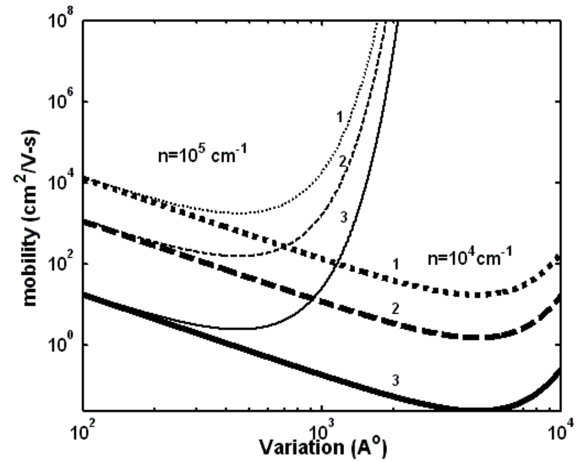

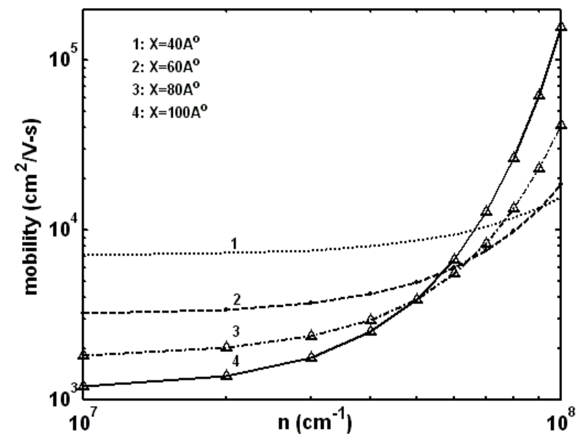

Fig. 6. (a) mobility μ as a function of d for different $X(=\Lambda)$ (b) mobility μ as a function of $X(=\Lambda)$ for two values of n equal to 10^4 cm^{-1} and 10^5 cm^{-1}. (c) mobility μ as a function of n for different $X(=\Lambda)$. Note, for all calculations, Δ is assumed to be 1nm.

In Figure 6(a), mobility vs. wire radius for different Λ is shown. Mobility is a very strong function of d (varies as d^6), and increases by an order of 10^6 as d increases by 10s of nanometers. This is expected because for the same amount of roughness along the edges, carriers scatter less if radius is more and hence, carrier mobility is larger. Scattering increases with increasing Δ and Λ and hence, mobility decreases, as is clear from Figure 6(a) & (b). From Figure 6(b) we can say that mobility first decreases and than increases as Λ is increased. Mobility attains a minimum value when Λ equals the Fermi wavelength (k_F^{-1}). This is because carriers scatter the most when Λ is very close to their wavelength. In Figure 6(c), mobility vs n is shown for different Λ. Mobility is very weakly dependent on n as long as carrier wavelength $\lambda < \Lambda$, and increases steeply as $\lambda > \Lambda$.

CONCLUSION

Hydrogenic impurity binding energy in a quantum wire has been studied as a function of the wire dimension and impurity position with respect to the wire axis. As the radius of the wire d increases, binding energy decreases. Maximum binding energy is obtained when impurity is located on the wire axis, and the minimum, when the impurity is at the boundary of the wire.

The electron carrier density is calculated from the impurity binding energy, which is a function of wire radius, temperature, and doping concentration. Carrier density increases when wire radius, temperature, and doping density increase. But, the impurity can not be ionized completely at room temperature as it can be in bulk crystals. Impurity ionization percentage decreases as doping density increases and temperature decreases.

The surface roughness limited momentum relaxation time has been derived by assuming a Gaussian distributive roughness along the surface of the nanowire. Mobility thus calculated varies strongly with d, as a function of d^6. Mobility first decreases, then increases as roughness variation Λ is increased, and reaches a maximum at the Fermi wavelength.

From our results, we propose the ideal condition for achieving high mobility in quantum wires as when d is sufficiently large and carrier wavelength λ is greater than Λ. Smaller Δ also improves mobility. Scattering limited mobility is of prime concern in very thin quantum wires. However, as d is made larger other scattering mechanisms like impurity scattering, become important and should be taken into account.

APPENDIX A

For the1-D case, the conduction band densities of states near the band edges can be expressed as:

$$g_c^{1D}(E) = \frac{\sqrt{2m_e^*}}{\pi\hbar}\frac{1}{\sqrt{E}},$$

and the number of electrons/cm with energies between E and $E+dE$ is $g_c(E)f(E)dE$. Then the total electron concentration in the conduction band is:

$$n^{1D} = \int_{E_c}^{E_{top}} g_c^{1D}(E)f(E)dE .$$

Under non-degenerate condition,

$$n^{1D} = \int_0^{\infty} \frac{\sqrt{2m_e^*}}{\pi\hbar}\frac{1}{\sqrt{xkT}}\exp(-\frac{E_c - E_F}{kT})\exp(-x)kTdx$$

$$= \frac{\sqrt{2m_e^* kT}}{\sqrt{\pi}\hbar}\exp(-\frac{E_c - E_F}{kT})$$

$$= N_C^{1D}\exp(-\frac{E_c - E_F}{kT}),$$

where $N_C^{1D} = \frac{\sqrt{2m_e^* kT}}{\sqrt{\pi}\hbar}$ is the 1-D effective density of conduction band states.

On the other hand, we can determine the degree of donor's ionization by

$$\frac{N_D^+}{N_D} = \frac{1}{1 + g_D \exp\frac{E_F - E_D}{kT}}$$

where g_D=2 (standard value)

Using the charge-neutral relationship for n-type material:

$$n \approx N_D^+,$$

we can get an equation for the electron concentration in the conduction band:

$$2n^2 + N_C\exp(-\frac{E_b}{kT})n - N_C N_D \exp(-\frac{E_b}{kT}) = 0,$$

where N_D, N_C and n all have the unit of 1/length. Then n can be solved.

APPENDIX B

Momentum relaxation time is given by,

$$\tau_m^{-1} = \sum_{k'} (N_I V) S(k,k')(1-\cos\theta)$$

where $S(k,k') = \frac{2\pi}{\hbar} \left|\langle k'|V(r)|k\rangle\right|^2 \delta(E_{k'} - E_k)$,

total carrier density $N_I V = nL$, n is carrier density (cm^{-1}) and L is the wire length. θ is the angle between the initial and final wavevectors k and k'. In the ground state, the carrier's motion is essentially along the wire's axis and hence θ can take only two values: zero for forward scattering (which doesn't contribute to the scattering rate) and π for backward scattering.

Calculation of Matrix elements:

$$\psi_{10k}(x) = \frac{e^{ikz} J_0(k_{10}\rho)}{(\pi d^2 L)^{1/2} J_1(k_{10} d)},$$

$$V(r) = -\frac{\hbar^2 (2.405)^2}{m^* d^3} S(r), \text{ and}$$

$$S(r) = \Delta \exp(-\frac{z^2}{\Lambda^2})$$

Using,

$$\tau_m^{-1} = \frac{4m^* L}{\hbar^3 k} \int_0^L \int_0^d N_{1D} (2\pi\rho d\rho) dz \left| \int_0^d \int_0^L \psi_{10}^* V(r) \psi_{10} 2\pi\rho d\rho dz \right|^2$$

$$= \frac{4m^* L}{\hbar^3 k} \frac{4\hbar^4 (k_{10} d)^4 \Delta^2}{m^* d^{10} L^2 J_1^4 (k_{10} d)} N_{1D} L \left[\int_0^d \rho d\rho J_o^2 (k_{10}\rho) \right]^2 \left[\frac{\sqrt{\pi}}{2} \Lambda e^{-k^2 \Lambda^2} \right]^2$$

and $k_{10}d$=2.405 (first root of $J_1(k_{10}d)$), which gives the final expression for τ_m^{-1}

ACKNOWLEDGEMENT

We would like to thank Dr. Debdeep Jena for his extensive support throughout the course of the project.

REFERENCE

1. G. E. Moore, *Electronics* **38**, 114 (1965)
2. S. Chau, *Intel Magazine*, (2004)
3. B. Doyle et al., *Intel Magazine*, (2003)
4. C. Dekker, *Phys. Today* **52** (5), 22 (1999)
5. A. Javey et al., *Nature* **424**, 654 (2003)
6. S. Heinze et al., *Phys. Rev. Lett.* **89**, 10:106801 (2002)
7. Y. Cui et el., *Nano Lett.* **3**, 149 (2003)
8. X. Duan et al. *Nano Lett.* **2**, 487 (2002)
9. C. A. Stafford, *Phys. Stal. Sol. (b)* **230**, No. 2, 481 (2002)
10. C. A. Stafford, *Phys. Rev. B* **68**, 165414 (2003)
11. W. E. Buhro and V. L. Colvin, *Nature Lett.* **2**, 138 (2002)
12. M. Beard et al., *Nano Lett.* **2**, 982 (2002)
13. M. Mohamed et al., *Nano Lett.* **1**, 589 (2001)
14. Y. Cui et al., *J. of Phys. Chem. B* **104**, 5213 (2000)
15. K. Liu, *Phys. Rev. B* 58, 14681 (1998)
16. D. D. D. Ma, *Science* **299**, 1874 (2003)
17. H. Sakaki, *Jpn. J. Appl. Phys* **19**, L735 (1980)
18. H. Sakaki, *J. Vac. Sci. Technol.* **19**, 148 (1981)
19. C. H. Mailhiot et al., *Phys Rev. B* **26**, 4449 (1982)
20. R. J. Elliot and R. Loudon, *J. Phys. Chem. Solids* **8**, 382, 421 (1959)
21. J. Lee and H. N. Spector, *J. Vac. Sci. Technol.* **B2**, 16 (1984)
22. J. W. Brown and H. N. Spector, *J. Appl. Phys* **59**, 1179 (1986)
23. J. W. Brown and H. N. Spector, *J. Vac. Sci. Technol. B* **4**, 453 (1986)
24. G. Bastard, *Phys. Rev. B* **24**, 4714 (1981)
25. U. Penner et al., *Semicond Sci. Tech.* **13** 709 (1998)
26. H. Sakaki et al., *Appl. Phys. Lett* **51***,* 1934 (1987).